Phosphorus recovery from high solid content liquid fraction of digestate using seawater bittern as the magnesium source

Pepè Sciarria T. [a*], Zangarini S. [a], Tambone F. [a], Trombino L. [b], Puig S. [c], Adani F. [a]

[a] Gruppo Ricicla, Lab. Agricoltura e Ambiente, Università degli Studi di Milano (DiSAA), Via Celoria 2, 20133 Milano, Italy.

[b] Università degli Studi Milano, Dip. Scienze della Terra "Ardito Desio", Milan, Italy

[c] LEQUIA, Institute of the Environment, University of Girona. C/ Maria Aurèlia Capmany, 69, E-17003 Girona, Spain.

* corresponding author, tommy.pepe@unimi.it

Abstract

Phosphorus recovery from digestate is considered a challenge because the possible discharge can lead to eutrophication. This study focuses on phosphorus recovery as struvite from the liquid fraction of swine manure digestate at a high total solids concentration, by using a lab-scale crystallizer operated in continuous mode (7 $L \cdot d^{-1}$). A by-product of salt production (seawater bittern, SWB) was assessed as Mg source for the formation of struvite instead of a chemical dosage ($MgCl_2$) within a circular economy approach. Different Mg/P (1.8:1; 2:1; 3:1) ratios and different TS contents (TS 3.5 and 4.5 %) were studied. The maximum P recovery of 85% and N recovery of 52 % was obtained at 4.5% of TS and Mg/P ratio of 2:1, corresponding to an overall P and N recovery on the raw digestate of 70% and 46%, respectively. The presence of struvite was confirmed by X-ray diffraction (XRD) and scanning electron microscopy (SEM-EDS). Dried samples were then used as fertilizer in agronomic pot tests using *Brassica rapa chinensis*. Struvite obtained, showed comparable fertilizing properties in comparison with

conventional fertilizers in terms of P (Mineral 5.6 ± 0.4; Poultry 5.7 ± 0.2; Struvite 5.9 ± 0.1 g kg^{-1}), N and total biomass content such as chlorophylls ratio. The growth tests confirmed the possible use of struvite recovered as competitive alternative to conventional chemical phosphate fertilizers. The results showed that it can be possible to promote sustainable P recovery from high solids digestates by the combination of crystallizer reactor and Mg-salt byproducts.

Keywords

Digestate; P recovery; Seawater bittern; Struvite.

1. Introduction

Since the world population will reach almost 9.3 billion in 2050 (United Nations, Department of Economic and Social Affairs, 2019; Bank et al., 2020) one of the direct consequences is the rise in food production and consumption by developing countries (FAO, 2017; Vaccari et al., 2018; United Nations, Department of Economic and Social Affairs, 2019; OECD-FAO Agricultural Outlook, Edition 2021).

The rising of food supply is kinked to a higher global demand for fertilizers that will be expected to reach 318.65 million tonnes by the end of 2022, with an average annual increase of 2 millions tonnes from 2020 to 2022 (FAO, 2019). These are worrying data both for the steady increase in demand for fertilizers and the potential pollutant nature of N and P in the environment (FAO, 2019) and one of the main target is to limit nutrient damage due to pollution caused by livestock effluents (Nitrates Directive 91/676/EE; Vaccari et al., 2018; Zangarini et al., 2020).

Unfortunately, the nitrogen targeted directives of the European Union (Nitrates Directive 91/676/EE) are insufficient for manure handling (Szogi et al., 2015); infact the unbalanced nitrogen-phosphorus ratio applied for crop production leads to a phosphorus excess in soils with

potential risks of water pollution (i.e. eutrophication) (Evanylo et al., 2008; Szogi et al., 2015; Zangarini et al., 2020).

The P pollution problem runs alongside the rising demand for phosphatic mineral fertilizers. World consumption of P_2O_5 contained in fertilizer and industrial uses was projected to increase to 52.5 million tons in 2024/2016 from 49.6 million tons in 2021 (IFA, 2021). To meet this demand, phosphorus is obtained from phosphate rocks, a limited and non-renewable source which is going to become less available from 2050 onwards (Ashley et al., 2011; Kataki et al., 2016a; Vaccari et al., 2018; U.S. Geological Survey, 2021). Moreover, Morocco holds 74% of the available global deposits of phosphate rock while the main quantities of phosphorus are mined in China and South Africa (Sørensen et al., 2015; Desmidt et al., 2015; Kataki et al., 2016ª; U.S. Geological Survey, 2021.).

Within a global scenario, Europe is the region most dependent on phosphorus imports due to a very low local phosphorus production and for this reason it must import 86% of its total demand (IFA, 2014). Consequently, the geopolitical situation can have a significant influence on the P price and availability (Guedes et al., 2014) leading to a possible global phosphorus crisis (Vaccari et al., 2018). At the same time, global human activity discharges annually 1.62 million tonnes of P into the major freshwater pools on Earth, surpassing on 38% of the land surface the planet's assimilation capacity (Mekonnen and Hoekstra, 2018; Vaccari et al., 2018; van Puijenbroek et al., 2019). This surplus input of phosphorus into natural water bodies could be extremely dangerous as described previously (Dyhrman et al., 2007; Seitzinger et al., 2010; Ashley et al., 2011). Several measures has been taken to overcome this environmental issue, such as an upgrade of the Urban Wastewater Treatment Directive 91/271 (UWWTD) (Council of the European Communities, 1991) and the Regulation n.259/2012 (European Parliament, 2012), which have led to developments in the European wastewater treatment system to adapt to new discharge regulations (Jaffer et al., 2002).

In consideration of these problems related to the phosphorus issue, strategies and technologies aimed to recover this key macronutrient represent one resolution to respond both to the forthcoming depletion of the fertilizer's supply and eutrophication problem. P-recovery processes are the most promising technologies to overcome these concerns achieving phosphorus-free effluents from wastewaters and which focus on by-products reusable for other purposes (Zangarini et al., 2020). Recycled P fertilizers from waste streams should increasingly replace mineral P fertilizers derived from phosphate rock. This requires further research on alternative fertilizers as well as their market approval for conventional and possibly also for organic farming. The specific characteristics of recycled P fertilizers have to be considered, in particular the short- and long-term availability of P contents and the concentrations of contaminants (Garske et al., 2020). Currently, urban and industrial sewage are the main targets for these processes, while there are limited approaches available for livestock manure treatment due to the ready availability of low-cost alternatives and the lack of suitable markets for processed residues (Vaccari et al., 2018). For example, dutch agricultural sector produces about 75 million kg P y^{-1} as animal manure of which 25% cannot be applied to land in the Netherlands because of P application limits for agricultural land (Zangarini et al., 2020). Take in to account the possibility to recover more than 90% of this discarded P (around 17 million kg P y^{-1}) by using the struvite crystallization approach and estimated that the importing of P mineral fertilizer into the Netherlands is about 7 million kg P y^{-1}, the recovery of P which cannot be applied as fertilizer in the Netherlands (i.e. 22% of the total 75 million kg P y^{-1} produced) could potentially replace the demand for P mineral fertilizer, removing both the problem of animal manure disposal and the import costs (Zangarini et al., 2020; Al-Mallahi et al., 2020).

In consideration of this issue and the potential impact of the P recovery from livestock manure, this study focuses on methods for phosphorus recovery by struvite precipitation starting from the digestate. In particular, phosphorus can be recovered from waste streams by the crystallization of struvite ($MgNH_4PO_4$), which is an effective slow-release fertilizer. Struvite offers many

advantages versus conventional fertilizers, such as low leach rates and slow release of nutrients. Nevertheless, livestock manure has a high total solids (TS) content (TS >5% DM) which seems to be one of the main limitations for the recovery of P from the influent solution by struvite crystallization (Yetilmezsoy et al., 2017; Tarragó et al., 2018) .

Struvite crystallizer technology has been developed in different prototypes and put into production successfully abroad. but few of them are not suitable for livestock effluents, due to high solids content (3-4 % TS) that influence the struvite crystallization process (Zangarini et al., 2020; Al-Mallahi et al., 2020). This study aims to elucidate and to overcome the effect of high solids content of livestock effluents (3-4% TS) on struvite formation during crystallization process using a complex matrix, such as digestate including the investigation of dry matter and P repartition during each step of the process. In particular, liquid fraction of digestate obtained after screw press separation in real scale biogas plant, was used as P source for crystallization; the liquid fraction was used according with previous data where was reported that the large parte of the initial P of the digestate was reparted in the liquid fraction after screw press separation (Tambone et al., 2017). Special attention is given to identify the role of solids in P recovery as struvite and its impact on the quality of the product recovered. In accordance with a circular economy approach, the crystallization processes was carried out using seawater bittern, i.e. an alternative Mg source, a by-product of sea salt production. Seawater bittern was used in order to decrease the cost of the process with respect to a conventional synthetic Mg sources (Zangarini et al., 2020). The entire process was set up in order to simulate a little lab-scale process able to recover P and N as struvite from a real digestate coming from a biogas plant by using a simple designed crystallizer reactor. Moreover, the liquid fraction of digestate was not diluted unlike the several papers reported in literarute (Tarragó et al., 2018; Wagner et al., 2022). Additionally, the struvite recovered in the crystallization process was used in an agronomic growth test to compare struvite's fertilization properties with those of conventional chemical P fertilizers.

2. Materials and methods

2.1 Crystallizer setup

A polymethylmethacrylate (PMMA) crystallizer was specifically designed to reproduce the optimal conditions for struvite precipitation. In detail, this prototype of an air-lift reactor (total volume 6.9 L) was differentiated into three zones: riser, clarifier, and collector (Fig. S1). The supersaturated condition of the riser zone ensured the struvite growth, enhanced by the recirculation and up-flow of small particles (centres of nucleation) (Tarragò et al., 2016). The clarifier section consisted of a quiet zone in which these particles rise and fall. In the collector, the nuclei settled once their settling velocity was higher than the up-flow velocity.

2.2 Influent solutions

Digestate (D) and derived liquid (LF) and solid (SF) fractions were collected from an anaerobic digestion plant in Lombardy Region. The plant was fed using swine manure and corn. The liquid fraction of swine digestates, separated by screw press, was used as the N and P source (Table 1) in the struvite crystallization process. The liquid fraction of digestate was used to test the influence of high total solids concentration (TS>3%) on struvite crystallization. Seawater bittern (SWB) was collected in the saltworks of Porto Viro (Compagnia Italiana Sali, Rovigo, Italy). Seawater bittern is a by-product of sea salt processing mainly composed of magnesium chloride (>95%). It is considered a low-cost magnesium source (Zangarini et al., 2020). SWB was used in the crystallization process, to substitute magnesium chloride as the Mg source.

The liquid fraction of digestate was filtered accordingly to achieve the desired concentration of solids and the influent SWB magnesium solution was dosed to get the specific Mg^{2+}/PO_4^{3-} molar ratios previously reported.

150 The separation efficiency between the solid (% SF) and the liquid fraction (% LF) on fresh
151 weight (FW) was calculated as previously described (Supporting information; Tambone et al.,
152 2017).
153
154 **2.3 Experimental design**
155 The liquid fraction of digestate (LFD), the P source, and seawater bittern solution (SWB), the
156 Mg source, were pumped in order to obtain an hydraulic retention time (HRT) fixed at 24 h, i.e.
157 6.9 L d^{-1}. In particular, the liquid fraction of digestate was fed continuously at 0.29 L h^{-1} and a
158 seawater bittern was fed continuously at 0.02 L h^{-1}. Magnesium was the limiting compound in
159 the influent. Sea water bittern (SWB) was added to allow struvite precipitation at different
160 Mg^{2+}/PO_4^{3-} molar ratios for each test (1.8:1, 2:1 and 3:1) according to data previously reported
161 (Tarragò et al., 2016; Tarragò et al., 2018). Aeration was applied in the riser zone and controlled
162 by a mass flow meter to maintain the up-flow rate desired. This velocity in the riser was related
163 to the size of particles (Supporting information; Tarragò et al., 2016). In all the tests up-flow
164 velocity and pH were the fixed parameters.
165 In the reactor, the up-flow velocity was kept constantly at 0.5 L min^{-1} employing a mass flow
166 meter to match the critical settling velocity of the particles in the liquid.
167 The operating pH in the reactor was constantly maintained between 8.5 and 9 with a solution
168 of NaOH 1 mol L^{-1} using a control panel.
169 The supersaturation (Sr) is the driving force for struvite formation. Sr was calculated based on
170 the methodology followed by Bergmans (2011) (Supporting information).
171 The first three tests, operated in continuous mode were carried out at the molar ratios of
172 Mg^{2+}/PO_4^{3-} of 1.8:1, 2:1 and 3:1 with a total solid (TS) content of the liquid digestate of 3%
173 (w/w) (Tests 1, 2 and 3) while the following two tests (Tests 4 and 5) were carried out with the
174 TS of 4.5% (w/w). The TS % were selected in order to use the TS % commonly found in the
175 liquid fraction of digestate of a real-scale biogas plant (Tambone et al., 2017). This was done

176 to find out the influence of these combined parameters on struvite formation. Struvite particles
177 settled in the collector zone of the crystallizer were daily recovered together with the effluent
178 wastewater.

179 **2.4 Measurements and chemical analyses**

180 Samples daily collected from during crystallization processes (125 ml d^{-1}) were dried for 24 h
181 at 40 °C (for crystals analysis) and then, for an additional 24 h at 105 °C (APHA, 1992). TS
182 were determined following standard procedure (APHA, 1992). Total Kjeldahl Nitrogen (TKN)
183 and Total Ammonia Nitrogen (TAN) were determined by using the analytical method for
184 wastewater sludge (IRSA CNR, 1994). Total P, Mg , Ca, K, Fe, contents were determined by
185 inductively coupled plasma mass spectrometry (Varian, Fort Collins, USA) preceded by acid
186 digestion (Tambone et al., 2007). Total organic carbon was analysed by dichromate methods
187 (APHA, 1998). All analysis were performed in triplicate. The same analysis were also
188 performed in the growth test (2.4) and chlorophyll was extracted by acetone (solution 80%) and
189 determined by spectrophotometer at 645 and 663 nm, for Chlorophyll A and B, respectively.
190 The struvite samples for bulk X-ray powder diffraction (XRD) were pulverized and measured
191 by a Bragg-Brentano geometry PANalytical X'Pert Powder Diffractometer, using CuKα
192 radiation (1.5417 Å) (40 kV and 40 mA), and a X'Celerator detector.
193 Optical microscope observations were made with a LEICA DM R optical microscope
194 (Germany) and images were acquired with a Leica EC3 camera and LAS V4.1 software.
195 Backscattered electron images of the struvite crystals were obtained using an electronic
196 scanning microscope (SEM) JEOL - JSM IT-500 with acceleration current of 1-30 kV,
197 Tungsten (W) filament and embedded EDS microprobe for chemical analyses.
198

199 **2.5 Growth tests**

To test the fertilizing performance of the struvite obtained (S), a growth test was carried out using as the test plants *Brassica rapa chinensis* (Hybrid F1 Green Rocket), which is sensitive to phosphate fertilization (van Averbeke et al., 2007). The test was performed comparing struvite (S) with a mineral fertilizer (Ca $(H_2PO4)_2$) (M) and with poultry manure (P). In addition, a non-fertilized control (∅) was included. Poultry manure was chosen because it contains P and organic matter, in analogy to the recovered struvite that also contained organic matter. The tests were carried out in triplicate in pots (1 L capacity) using peat at a pH of 5.6 as a growth medium. The plants were grown for 40 days in a phytotron at an average temperature of 25 ° C during the hours of light and 20 ° C in the hours of darkness (16 hours of light and 8 hours of darkness), keeping them at a soil humidity equal to 60% of the water holding capacity. For each treatment 0.322, 0.169 and 1.245 g pot^{-1} of N, P_2O_5 and K_2O were added to each pot, which corresponded to 160-120-120 kg Ha^{-1} of N, P_2O_5 and K_2O. To balance N and K, urea and potassium sulphate salts were also used (Supporting information Tab. S1). At the end of the test, the plants were collected and weighed to determine the fresh weight. The chlorophyll content was determined on the fresh leaves. Finally, the plants were placed in a ventilated oven at 65 ° C to obtain dry samples to analyse phosphorus and nitrogen content.

2.6 Statistical analyses

The comparisons between the agronomic performances of the groth test were carried out through One-way ANOVA analysis, with Tukey post-test. Unless otherwise specified, the significance limit value p was set at 0.05 for all the analyses carried out. The statistical analyses were carried out using IBM SPSS® 23 software (version 16) (SPSS, Chicago, IL). The plots were obtained through the use of Microsoft EXCEL 2016.

3. Results and discussion

3.1 Crystallizer precipitation tests

Different crystallization conditions were tested to achieve a stable high P removal value over time. In all tests, the steady-state P removal was achieved after approximately 5-10 days (start-up) which was in line with previous results reported in the literature (Tarragò et al., 2018). Table 2 summarises the overall results, i.e. the P-removal efficiencies achieved at stable conditions for each test. During Test 1, using a Mg^{2+}/PO_4^{3-} molar ratio of 1.8:1 and a TS content of 3.5 ± 0.2% ww, a P recovery of 57.9 ± 6.2% total P (Ptot) was obtained while the N recovery was of 46 ± 4.2 % total N (TKN). In Test 2, Mg^{2+}/PO_4^{3-} molar ratio was increased to 2:1 while TS content was maintained at 3.5 ± 0.2% ww. In this case, the P recovery efficiency was higher than Test 1, achieving 84.2 ± 1.9% Ptot and 52 ± 3.2 % of TKN, respectively. In Test 3, the Mg^{2+}/PO_4^{3-} molar ratio was changed to 3:1 maintaining the same TS content (3.5 ± 0.2%). In this case, 71.7 ± 6.6% of Ptot removal and the 31 ± 4.7% of TKN removal were achieved. After these trials, the effect of increasing the TS content to 4.5% ± 0.2% to the crystallization process was studied. Tests 4 and 5 were conducted to simulate the input of raw digestate (without any filtration) in the crystallizer reactor. During Test 4, the Mg^{2+}/PO_4^{3-} molar ratio was fixed at 2:1 reaching Ptot removal of 76 ± 5.1% with a simultaneous N removal of 38.9 ± 2.1% TKN. The Mg^{2+}/PO_4^{3-} molar ratio was increased to 3:1 in Test 5. The respective P and N removal efficiencies were of 60.5 ± 1.8 % Ptot and 33 ± 3.6% TKN. In these two last tests, the removal efficiency was lower than in Tests 2 and 3, probably because of the high amounts of total solids (TS >4%) and organic matter that may limit the amount of struvite crystallized (Havukainen et al., 2016). Nevertheless, the result obtained during Test 4, was higher than Test 3 even though the content of solids was higher. To better understand the value of the results achieved, data acquired were compared with those reported in the literature. For example, Tarragò et al. (2018) were able to reduce P concentration in digestate from pig slurry from ~370 mg PO_4^{3-} L^{-1} to ~15 mg PO_4^{3-} L^{-1}, i.e. 95% recovery efficiency, but by using a significantly lower concentration of TS (0.1-0.3 %) in comparison to this work. Qureshi et al. (2008) reported a P recovery of up to

90% from digested manure (initial TS content 1.5 %) but only after microwave and peroxide treatment that led to a TS reduction of 0.26 % that was several times lower than TS concentration used in this work. As shown previously, the results achieved in this work were in line with those reported in the literature unless high TS were investigated. We focused on the possibility of using digestate from manure which had high TS in the P recovery crystallization process without dilution or massive filtration that could make the process unfeasible on a full-scale level (Zangarini et al., 2020).

As shown previously, the best P removal efficiencies were reached in Tests 2 and 4, respectively representative of low (3.3%) and high (4.5%) TS content, and with Mg^{2+}/PO_4^{3-} molar ratio in the reactor 2:1 (Table 2). Therefore, samples collected during Tests 2 and 4 were chemically characterized to evaluate the nutrients content (Table 3); since these tests showed the best performance in P removal they were used as starting point to calculate the ripartition of dry matter in the entire system and to evaluate the fertilizing properties of the products obtained from crystallization; for this reason the rest of the work was focused on tests 2 and 4. The collected samples showed a higher Ptot concentration, 46 ± 4.7 g kg^{-1} of TS and 55.2 ± 3 g kg^{-1} of DM for Tests 2 and 4, respectively, than the initial liquid fraction of digestate inlet into the crystallizer (sample F; Table 1). This confirmed the possibility to recover P by using this crystallization method. The same trend was also observed taking into account the C content in samples collected in Test 2 (42.1 ± 1.3 g kg^{-1} of TS) and Test 4 (29.6 ± 2.1 g kg^{-1} of TS).

The collected particles were then used as fertilizer in the growth test as described in section 3.3.2.

3.2 Repartition of total solids phosphorus and nitrogen

To understand the overall removal efficiency of the system proposed, the repartition of nutrients and total solids from the digestate to the crystallizer's effluent was calculated. Data reported in Table 1 show the repartition of the total solids in all solid and liquid fractions determined by

using Eq. 3 (Supporting information). An average of 17.1% of the total DM of digestate moved to the solid fraction (SF) and the 82.9% (on average) remained in the liquid fraction (LF) (see Figures 1 and 2). In Test 2, the filtration of the LF

led to another separation of the dry matter: 9.5% (on average) of the LF dry matter went to the filtration residue (FR), while the 73.4% remained in the filtered liquid (F).

Based on the DM breakdown, the repartition of total P and TKN was then estimated, from the initial digestate to the final output of the crystallizer (Fig. 1). 70 % of total P and 46 % of TKN of the digestate ran out of the collector during the maximum efficiency interval of Test 2 (crystallizer internal removal efficiency: 84.2 ± 1.9%) (Fig. 1).

In Test 4, 75.4% (as average) of the digestate total DM went in the raw material lightly filtered (F), while the remaining 7.5% went in the FR (Fig. 2). Considering that in Test 4 the highest crystallizer internal efficiency was 76 ± 5.1%, it was then estimated that 65 % of total P and the 34% of TKN of the digestate ran out of the collector. The results achieved during sections 3.1 and 3.2 showed the possibility to recover up to 70-80% of the total P from high solid content slurry, such as digestate; moreover, the large part of the initial total P moved from the digestate to the liquid fraction and then to the filtrate used in the crystallization (Fig.1 and Fig. 2) as espected (Tambone et al., 2017, Guilayn et al., 2019b; Zangarini et al., 2020). According with these results, the system proposed in this paper, i.e. separation and crystallization, seems to have the charateristics in terms of P recovery efficiency and in easily up-gradable design that could lead to a real scale process able to treat high solids slurries (Zangarini et al., 2020). In facts, screw press separation is one of the most common and cheap method to perform liquid/solid separation of the digestate after the AD process (Guilayn et al., 2019b) and the crystallizer reactor is one of the most promising design to enhance P recovery at the pilot, and commercial scale together with the use of low-cost Mg source (Peng et al., Krishnamoorthy et al., 2021).

3.3 Characterization of the recovered product

3.3.1 X-ray diffraction (XRD) analyses and Scanning Electron Microscope (SEM) Analyses

304 The grown crystals of Tests 2 and 4 were analyzed by X-ray diffraction (XRD). This method
305 was performed to quantitatively determine the crystal phases and amorphous content of struvite
306 samples. As shown in Figure 3, XRD analyses exhibited several peaks indicative of the presence
307 of struvite in the collector samples. In particular, the samples corresponding to the highest P
308 removal in Tests 2 and 4 (Figure 3; Figure S2; Figure S3) showed the exclusive presence of
309 struvite crystals together with potassium chloride and magnesium calcite, but without the
310 presence of other P salts crystals. Nevertheless, Test 2 showed a high amorphous content, i.e.
311 the curved baseline (Fig 3). The amorphous part of the precipitated particles can also contain
312 several P amorphous compounds such as amorphous struvite, amorphous hydroxyapatite or
313 calcium phosphate that can contribute to the overall P recovery as expected (Tarragò et al.,
314 2018).

315 This hypothesis could be confirmed by the analysis of the collected samples (Table 3);
316 calculating the numbers of moles from the number of elements identified in Test 2 (Table 3)
317 the Mg/P ratio was 1:2.4, which was far from the theoretical Mg/P ratio present in struvite
318 crystals (Mg/P=1:1) (Zangarini et al., 2020) confirming the presence of other P amorphous
319 compounds (Tarragò et al., 2018). Test 4 showed a remarkable presence of quartz, probably
320 due to the high concentration of TS (4.5 %) (Jimenez et al., 2020) (Fig. 3) . Nevertheless, the
321 quality of the struvite recovered was not influenced by the concentration of TS at 4.5%. In this
322 case, the amorphous baseline was flatter than in Test 2, indicating a lower presence of
323 amorphous compounds (Figure 3). This was remarked by the calculation of Mg/P molar ratio
324 of recovered product that was around 1:1, very close to the stoichiometry Mg/P ratio present in
325 struvite crystals (Table 3). The lower presence of P amorphous compounds did not influence
326 significantly the amount of P recovered; in Test 4, 76 ± 5.1% of P removal was observed (Table
327 2). SEM observations coupled to EDS analyses were performed on recovered products of Test
328 2 and Test 4 to check the aspect (i.e. crystallinity) of struvite crystals. It appears that the coarser

329 and better-formed struvite crystals are easier to distinguish and to identify in Test 4 samples
330 (Figure 4 - the size of crystals is a few tens of micrometres).

331

332 ***3.3.2 Agronomic growth tests***

333 Agronomic tests were performed to assess the fertilizing properties of the final product
334 collected in Tests 2 and 4 in comparison with the performances of common mineral phosphatic
335 fertilizers and poultry manure. The tests were conducted using *Brassica rapa chinensis* (cv.
336 Green Rocket).
337 The results showed, as expected, a significant difference between the samples grown with no
338 added fertilizers (control samples; Ø) and the others cultivated with struvite collected (S),
339 poultry manure (P) and common mineral fertilizers (M), respectively (Figure S4). As described
340 in Table 3, plants fertilized with struvite showed an amount of biomass of 50.9 ± 6.9 g pot^{-1}
341 that was higher than for plants fertilized with mineral fertilizer but lower than that for plants
342 grown with the addition of poultry manure. To evaluate nutrients adsorption, plants were also
343 analysed for TKN and Ptot content. In this case, plants fertilized with struvite showed a higher
344 TKN content (62.3 ± 3.0 g kg^{-1}; Table 3) compared to plants fertilized with poultry and mineral
345 fertilizer, respectively. A similar trend was observed analysing Ptot content (Table 3), the same
346 amount of Ptot was found in all plants.
347 Chlorophylls A and B are two fundamental pigments for plant photosynthesis. In chloroplasts,
348 the ratio of chlorophyll A to B is approximately 3:1. The total amount of both chlorophylls is
349 reported in Table 4; as shown by the data acquired, the proportion between chlorophyll A and
350 chlorophyll B was approximately 3:1, which was in line with the typical Chl A to B ratio of
351 *Brassica rapa chinensis* (Jiao et al., 2004). In plants fertilized with struvite, poultry manure and
352 mineral fertilizer, the ratios of the chlorophylls were almost the same. The statistical analysis
353 confirmed that the differences between the three different fertilizers were not significant, except

for the treatment with struvite where chlorophyll B was somewhat higher. The control samples showed a lack of nutrients (nitrogen content), low heights and less vivid colours in the leaves, in comparison with the fertilized plants (Figure S4). In particular, samples fertilized with struvite showed higher nitrogen and chlorophyll content. This was presumably due to the organic fraction included in the struvite collected during the tests in the reactor, which allows higher efficiencies in cultivation, as expected (Feifei et al., 2011).

4. Conclusions

P recovery from the liquid fraction of digestate by struvite crystallization was investigated. This study shows the possibility to recover the P form digestate up to 80% from the initial concentration by struvite crystallization even using digestate at high total solids concentration (TS>4%). Furthermore, the results achieved, indicated that sea-water bittern can be a low-cost alternative Mg source, leading to a high P recovery efficiency at both Mg:PO_4 2:1 and 3:1 molar ratios. The recovered crystals were composed mainly of struvite without the presence of other kinds of P crystals and at the same time, a little precipitation of amorphous P compounds. Agronomic tests with *Brassica rapa chinensis* confirmed the possibility of using the struvite produced as a competitive alternative to conventional chemical phosphate fertilizers. In conclusion, seawater bittern is a low cost alternative in comparison with the conventional Mg source for struvite precipitation, even using digestate at relatively high solid content; moreover,the simple design of the lab-scale crystallizer could be easily up graded to a real scale reactor that could work together with a biogas plant to recover the P present in the outflow digestate. Last, the application of struvite crystals as fertilizer can increase the downstream transferability of the process. In addition, struvite recovery using low-cost magnesium sources could be a way to mitigate future runoff due to the slow-release and lower water dissolution properties of this natural fertilizer product, thus reducing water contamination pressures.

Credit authorship contribution statement

Tommy Pepè Sciarria: Conceptualization, Methodology, Investigation, Data curation, Validation, Writing – original draft, Visualization. Sara Zangarini: Methodology, Investigation, Visualization, Writing – original draft. Fulvia Tambone: Conceptualization, Methodology, Investigation, Data curation, Writing – original draft, Supervision. Luca Trombino: Investigation, Data curation. Sebastià Puig: Conceptualization, Methodology. Fabrizio Adani: Conceptualization, Resources, Supervision, Validation, Writing – original draft, Project administration, Funding acquisition

.

Declaration of Competing Interest

The authors declare that they have no known competing financial interests or personal relationships that could have appeared to influence the work reported in this paper.

Acknowledgements

This work was supported by Gruppo Ricicla Labs, University of Milan (Università degli Studi di Milano), Italy, project No. 14135RV PRO RIC16FADAN02 M.

S.P. is a Serra Hunter Fellow (UdG-AG-575) and acknowledges the funding from the ICREA Academia award.

References:

Al-Mallahi, J., Sürmeli, R.O., Çalli, B.¸2020. Recovery of phosphorus from liquid digestate using waste magnesite dust. J. Clean. Prod. 272, 122616. https://doi.org/10.1016/j.jclepro.2020.122616

APHA, 1998. Standard Methods for the Examination of Water and Waste Water. American Public Health Association APHA-American Public Health Association,

403 1998. Standard Methods for the Examination of Water and Wastewater. 20th ed.
404 APHA. Washington. DC.

405 Ashley, K., Cordell, D., Mavinic, D., 2011. A brief history of phosphorus: From the
406 philosopher's stone to nutrient recovery and reuse. Chemosphere 84, 737–746.
407 https://doi.org/10.1016/j.chemosphere.2011.03.001

408 Bank, M.S., Metian, M., Swarzenski, P.W., 2020. Defining Seafood Safety in the
409 Anthropocene. Environ Sci Technol 54(14), 8506-8508.
410 https://doi.org/10.1021/acs.est.0c03505

411 Council of the European Communities, 1991. Directive concerning the collection, treatment
412 and discharge of urban wastewater and the discharge of wastewater from certain
413 industrial sectors (91/271/EEC). Off J Eur Communities Ser L 135–140.

414 Desmidt, E., Ghyselbrecht, K., Zhang, Y., Pinoy, L., Van Der Bruggen, B., Verstraete, W.,
415 Rabaey, K., Meesschaert, B., 2015. Global phosphorus scarcity and full-scale P-recovery
416 techniques: A review. Crit. Rev. Environ. Sci. Technol. 45, 336–384.
417 https://doi.org/10.1080/10643389.2013.866531

418 Dyhrman, S.T., Mooy, V., Devol, A., 2007. Microbes and the Marine Phosphorus Cycle.
419 Oceanography 20, 110–116.

420 Eurostat - Statistic explained, n.d. No Title [WWW Document]. URL
421 https://ec.europa.eu/eurostat/statistics-explained/index.php/Main_Page

422 Evanylo, G., Sherony, C., Spargo, J., Starner, D., Brosius, M., Haering, K., 2008. Soil and
423 water environmental effects of fertilizer-, manure-, and compost-based fertility practices
424 in an organic vegetable cropping system. Agric. Ecosyst. Environ. 127, 50–58.
425 https://doi.org/https://doi.org/10.1016/j.agee.2008.02.014

426 FAO, 2017. World fertilizer trends and outlook to 2018. Food Agric. Organ. United Nations
427 66.

428 Feifei, T., Qing, T., Fang, L., Bo, Y.,2 011. Kinetics of Phosphorus Removal and Recovery as

Struvite from Wastewaters with Medium-low Phosphorous Concentration. Energy Procedia, 11, 4528 – 4535.

Fleming, R., Ford, M., 2001. Human versus Animals - Comparison of Waste Properties. Beef 8–11.

Garske, B., Stubenrauch, J., Ekardt, F., 2020. Sustainable phosphorus management in European agricultural and environmental law. Reciel. 29, 107–117. Doi: 10.1111/reel.12318

Guedes, P., Couto, N., Ottosen, L.M., Ribeiro, A.B., 2014. Phosphorus recovery from sewage sludge ash through an electrodialytic process. Waste Manag. 34, 886–892. https://doi.org/https://doi.org/10.1016/j.wasman.2014.02.021

Guilayn, F., Jimeneza, J., Rouez M., Crest, M., Patureau D. 2019b. Digestate mechanical separation: Efficiency profiles based on anaerobic digestion feedstock and equipment choice. Bioresour. Technol. 274, 180–189. https://doi.org/10.1016/j.biortech.2018.11.090

Havukainen, J., Nguyen, M.T., Hermann, L., Horttanainen, M., Mikkilä, M., Deviatkin, I., Linnanen, L., 2016. Potential of phosphorus recovery from sewage sludge and manure ash by thermochemical treatment. Waste Manag. 49, 221–229. https://doi.org/https://doi.org/10.1016/j.wasman.2016.01.020

IFA, 2014. Fertilizer Outlook 2014-2018. 82nd IFA Annu. Conf. Sydney 1–7.

IRSA-CNR, Metodi analitici per le acque, 1994

Jadhav, D.A., Ghosh Ray, S., Ghangrekar, M.M., 2017. Third generation in bio-electrochemical system research – A systematic review on mechanisms for recovery of valuable by-products from wastewater. Renew. Sustain. Energy Rev. 76, 1022–1031. https://doi.org/https://doi.org/10.1016/j.rser.2017.03.096

Jaffer, Y., Clark, T.A., Pearce, P., Parsons, S.A., 2002. Potential phosphorus recovery by struvite formation. Water Res. 36, 1834–1842. https://doi.org/10.1016/S0043-

1354(01)00391-8

Jiao, S., Hilaire, E., Avelina Q. Paulsen and James A. Guikema* 2004Brassica rapa plants adapted to microgravity with reduced photosystem I and its photochemical activity Physiol. Plant.122, 281–290. doi: 10.1111/j.1399-3054.2004.00400.x

Jimenez, J., Grigatti, M., Boanini, E., Patureau, D., Bernet, N., 2020. The impact of biogas digestate typology on nutrient recovery for plant growth: Accessibility indicators for first fertilization prediction. Waste Manag. 117, 18-31. doi: 10.1016/j.wasman.2020.07.052.

Kataki, S., West, H., Clarke, M., Baruah, D.C., 2016a. Phosphorus recovery as struvite from farm, municipal and industrial waste: Feedstock suitability, methods and pre-treatments. Waste Manag. 49, 437–454. https://doi.org/10.1016/j.wasman.2016.01.003

Krishnamoorthy, N., Dey, B., Unpaprom, Y., Ramaraj, R., Maniam, G.P., Govindan, N., Jayaraman, S., Arunachalam, T., Paramasivan, B., 2021. Engineering principles and process designs for phosphorus recovery as struvite: A comprehensive review. J. Environ. Chem. Eng. 9, 105579 https://doi.org/10.1016/j.jece.2021.105579

Mekonnen, M.M., Hoekstra, A.Y., 2018. Global Anthropogenic Phosphorus Loads to Freshwater and Associated Grey Water Footprints and Water Pollution Levels: A High-Resolution Global Study. Water Resour. Res. 54, 345–358. https://doi.org/10.1002/2017WR020448

Nakakubo, T., Tokai, A., Ohno, K., 2012. Comparative assessment of technological systems for recycling sludge and food waste aimed at greenhouse gas emissions reduction and phosphorus recovery. J. Clean. Prod. 32, 157–172. https://doi.org/https://doi.org/10.1016/j.jclepro.2012.03.026

Nghiem, L.D., Koch, K., Bolzonella, D., Drewes, J.E., 2017. Full scale co-digestion of wastewater sludge and food waste: Bottlenecks and possibilities. Renew. Sustain. Energy Rev. 72, 354–362. https://doi.org/https://doi.org/10.1016/j.rser.2017.01.062

Nitrates Directive 91/676/EE; No L 375 / 4 Official Journal of the European Communities 31 . 12. 91

Parliament, E.U., 2012. REGULATION (EU) No 259/2012. Off. J. Eur. Union 94, 16–21.

OECD-FAO Agricultural Outlook, Edition 2021. http://dx.doi.org/10.1787/agr-outl-data-en.

Peng, L., Dai, H., Wu, Y., Peng, Y., Lu, X., 2018. A comprehensive review of phosphorus recovery from wastewater by crystallization processes. Chemosphere 197, 768-781. https://doi.org/10.1016/j.chemosphere.2018.01.098

Qureshi, A., Lo, K.V., Liao, P.H., 2008. Microwave treatment and struvite recovery potential of dairy manure. J. Environ. Sci. Heal. B 43, 350357

Seitzinger, S.P., Mayorga, E., Bouwman, A.F., Kroeze, C., Beusen, A.H.W., Billen, G., Van Drecht, G., Dumont, E., Fekete, B.M., Garnier, J., Harrison, J.A., 2010. Global river nutrient export: A scenario analysis of past and future trends. Global Biogeochem. Cycles 24. https://doi.org/10.1029/2009GB003587

Sørensen, B.L., Dall, O.L., Habib, K., 2015. Environmental and resource implications of phosphorus recovery from waste activated sludge. Waste Manag. 45, 391–399. https://doi.org/https://doi.org/10.1016/j.wasman.2015.02.012

Szögi, A.A., Vanotti, M.B., Hunt, P.G., 2015. Phosphorus recovery from pig manure solids prior to land application. J. Environ. Manage. 157, 1–7. https://doi.org/10.1016/j.jenvman.2015.04.010

Szogi, A.A., Vanotti, M.B., Ro, K.S., 2015. Methods for Treatment of Animal Manures to Reduce Nutrient Pollution Prior to Soil Application. Curr. Pollut. Reports 1, 47–56. https://doi.org/10.1007/s40726-015-0005-1

Tambone, F., Orzi, V., D'Imporzano, G., Adani, F., 2017. Solid and liquid fractionation of digestate: Mass balance, chemical characterization, and agronomic and environmental value. Bioresour. Technol. 243, 1251–1256. https://doi.org/10.1016/j.biortech.2017.07.130

506 Tarragó, E., Puig, S., Ruscalleda, M., Balaguer, M.D., Colprim, J., 2016. Controlling struvite
507 particles' size using the up-flow velocity. Chem. Eng. J. 302, 819–827.
508 https://doi.org/10.1016/j.cej.2016.06.036
509 Tarragó, E., Sciarria, T.P., Ruscalleda, M., Colprim, J., Balaguer, M.D., Adani, F., Puig, S.,
510 2018. Effect of suspended solids and its role on struvite formation from digested manure.
511 J. Chem. Technol. Biotechnol. https://doi.org/10.1002/jctb.5651
512 United Nations, Department of Economic and Social Affairs, P.D., 2019. No Title [WWW
513 Document]. URL http://www.un.org/en/development/desa/population/
514 Vaccari, D., Daneshgar, S., Callegari, A., Capodaglio, A.G., 2018. The Potential Phosphorus
515 Crisis : Resource Conservation and Possible Escape Technologies : A Review. Resources
516 7, 37. https://doi.org/10.3390/resources7020037
517 van Averbeke, W., Juma, K.A. and Tshikalange, T.E., 2007. Yield response of African leafy
518 vegetables to nitrogen, phosphorus and potassium: The case of Brassica rapa L. subsp.
519 chinensis and Solanum retroflexum Dun. Water Sa. 3, 355-362. DOI:
520 10.4314/wsa.v33i3.180595
521 van Puijenbroek, P.J.T.M., Beusen, A.H.W., Bouwman, A.F., 2019. Global nitrogen and
522 phosphorus in urban waste water based on the Shared Socio-economic pathways. J.
523 Environ. Manage. 231, 446–456 https://doi.org/10.1016/j.jenvman.2018.10.048
524 Wagner, E., Karthikeyan, K.G., 2022. Precipitating phosphorus as struvite from
525 anaerobically-digested dairy manure. J. Clean. Prod. 339, 130675.
526 https://doi.org/10.1016/j.jclepro.2022.130675
527 Yetilmezsoy, K., Ilhan, F., Kocak, E., Akbin, H.M., 2017. Feasibility of struvite recovery
528 process for fertilizer industry: A study of financial and economic analysis. J. Clean.
529 Prod. 152, 88–102. https://doi.org/10.1016/j.jclepro.2017.03.106
530 Zangarini, S., Pepè Sciarria, T., Tambone, F., Adani, F., 2020. Phosphorus removal from
531 livestock effluents: recent technologies and new perspectives on low-cost strategies.

Environ. Sci. Pollut. Res. 27, 5730–5743. https://doi.org/10.1007/s11356-019-07542-4

Zhang, H., Johnson, G., Fram, M., 2003. Managing Phosphorus from Animal Manure. http://osufacts.okstate.edu

Table 1. Chemical characterization of the digestate and the repartition of the total solid.

Samples	**TS**[a] (g kg^{-1} FM)	**TS** repartition (% TS)	**P_{tot}**[b] (g kg^{-1} TS)	**P_{tot}** repartition (% TS)	**TKN**[c] (g kg^{-1} TS)	**TKN** Repartition (%TS)	**TOC**[d] (g kg^{-1} TS)
D[e]	4.6 ± 1.2	100	28.3 ± 2.2	100	126 ± 1	100	2.4 ± 0.5
SF	185 ± 2.2	17.1	13 ± 2.4	9.7	32.6 ± 0.4	5.9	10.7 ± 1.5
LF	4.4 ± 0.3	82.9	25 ± 0.5	90.3	104 ± 0	94.1	2.7 ± 0.4
FR	97 ± 0.3	12.9	14.4 ± 1.7	8.9	58.8 ± 0.5	6.8	4.6 ± 0.6
F	33 ± 0.4	70	24.2 ± 1.8	81.4	139 ± 0	88.2	1.6 ± 0.7

[a]TS: Total solids;

[b]P_{tot} : total phosphorus

[c]TKN: Total Kjeldhal Nitrogen;

[d]TOC: Total Organic Carbon.

[e]D: Digestate; SF: Solid Fraction; LF: Liquid Fraction; FR: Filtration Residue; F: Filtrate

Table. 2 Crystallizer phosphorus removal efficiency for each test (average ± standard deviation).

Test	Mg^{2+}:P	TS[a] (%)	P Removal efficiency (%)	N removal efficiency (%)
1	1.8:1	3.5 ± 0.2	57.9 ± 6.2	46 ± 4.2
2	2:1	3.5 ± 0.2	84.2 ± 1.9	52 ± 3.2
3	3:1	3.5 ± 0.2	71.7 ± 6.6	31 ± 4.7
4	2:1	4.5 ± 0.2	76 ± 5.1	38.9 ± 2.1
5	3:1	4.5 ± 0.2	60.5 ± 5.8	33 ± 3.6

[a]TS: Dry Matter; the P and N removal efficiency were calculated as difference between the inlet and outlet solution after crystallization

Table 3. Chemical characterization of the collected samples from Tests 2 and 4 (average ± standard deviation).

Sample	**TS**[a] (g kg^{-1} FM[e])	**P_{tot}**[b] (g kg^{-1} TS)	**TKN**[c] (g kg^{-1} TS)	**TOC**[d] (g kg^{-1} TS)	**Mg** (g kg^{-1} TS)	**Ca** (g kg^{-1} TS)	**K** (g kg^{-1} TS)	**Fe** (g kg^{-1} TS)
Test 2	38.6 ± 0.8	46 ± 4.7	92.3 ± 4.1	42.1 ± 1.3	15.2 ± 2.2	41 ± 1	47 ± 0.9	3.4 ± 0.2
Test 4	71 ± 0.9	55.2 ± 3	62 ± 2.7	29.6 ± 2.1	36.2 ± 4.2	54.1 ± 1.7	21 ± 3.4	4.7 ± 0.9

[a]TS: Dry Matter;

[b]P_{tot} : total phosphorus

[c]TKN: Total Kjeldhal Nitrogen;

[d]TOC: Total Organic Carbon;

[e]FM: Fresh matter

614 Table 4. Agronomic performances (average ± standard deviation) Ø: control samples, no
615 fertilizers added; M: samples with mineral fertilizer added; P: samples fertilized with poultry
616 manure; S: samples fertilized with the collected struvite. Values of the same column followed
617 by different letters are statistically different ((*n*=3;P < 0.05 Tukey test).

Samples	Biomass/vessel (g)	TKN[iii] (g kg^{-1})	P_{tot}[iii] (g kg^{-1})	Clorophyll a (mg g^{-1})	Clorophyll b (mg g^{-1})
Ø[i]	22.9 ± 1.14a[ii]	19.8 ± 0.7a	1.1 ± 0.1a	817 ± 66a	286 ± 29a
M	42.1 ± 5.3b	56.6 ± 0.9b	5.6 ± 0.4b	1520 ± 12b	478 ± 1b
P	60.9 ± 5.6c	51.3 ±7.4b	5.7 ± 0.2b	1498 ± 189b	497 ± 57b
S	50.9 ± 6.9bc	62.3 ± 3.0c	5.9 ± 0.1b	1565 ± 91b	522 ± 39b
p	p < 0.05	p < 0.05	p < 0.05	p < 0.05	p < 0.05

618 [i] Ø control samples, no fertilizers added; M: samples with mineral fertilizer added; P: samples
619 fertilized with poultry manure; S: samples fertilized with the collected struvite.
620 [ii] Values of the same column followed by different letters are statistically different (p < 0.05
621 Tukey test).
622 [iii] TKN= Total Kjeldahl Nitrogen: Ptot= total Phosphorous

623

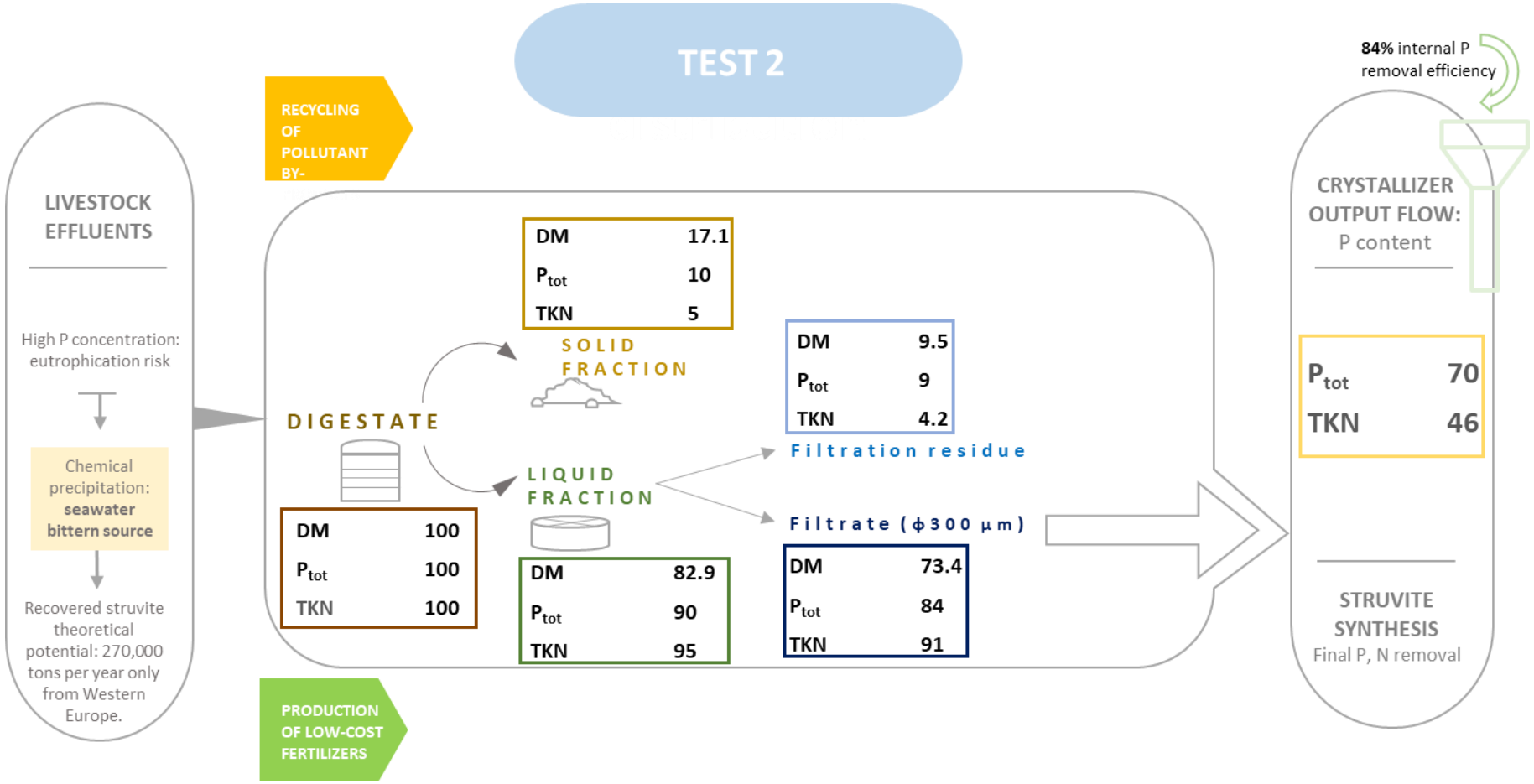

624

625

626 Figure 1. Mass balance for Test 2. DM: dry matter. The number are referred to % .

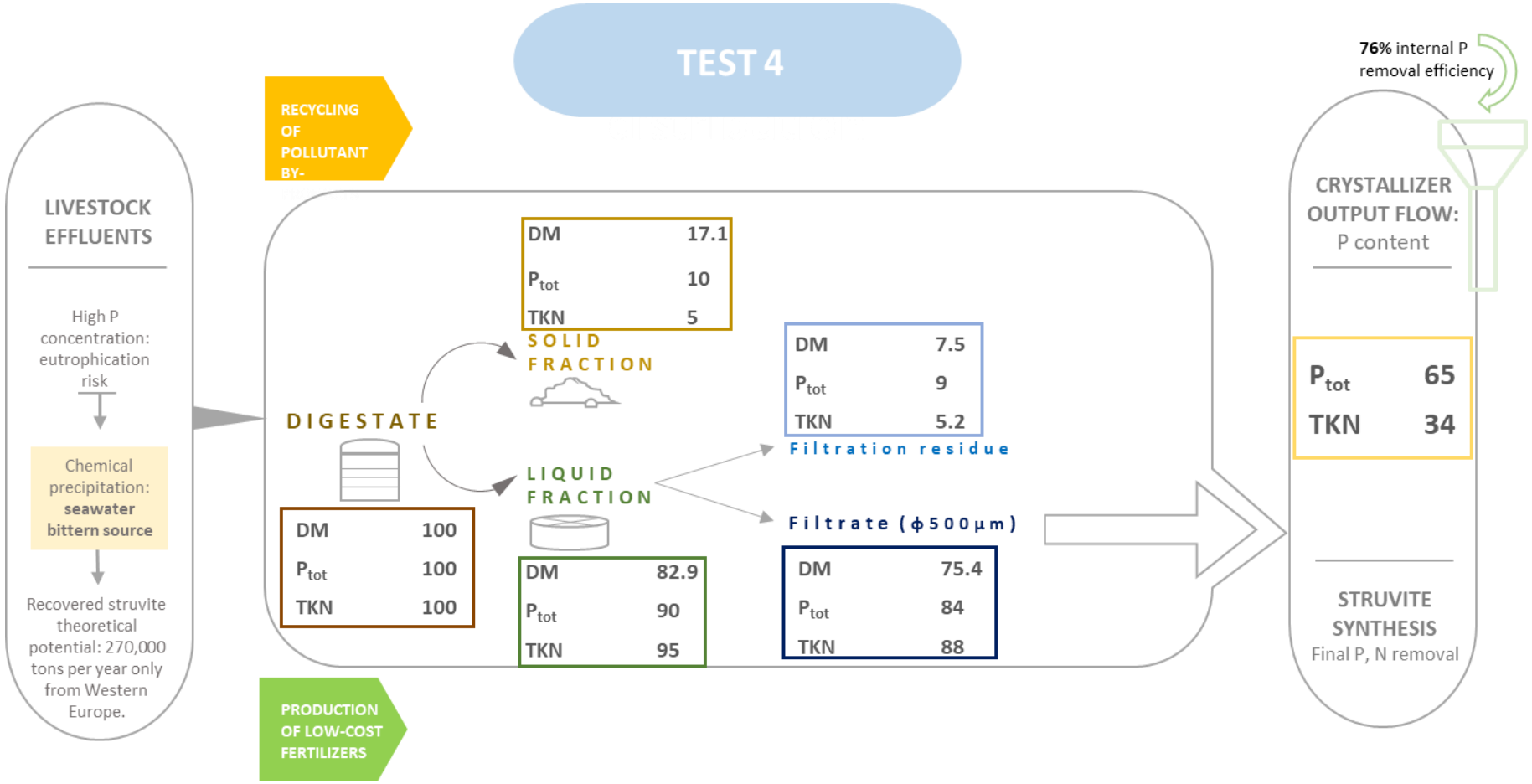

627

628

629 Figure 2. Mass balance for Test 4. DM: dry matter. The number are referred to % .

630

631

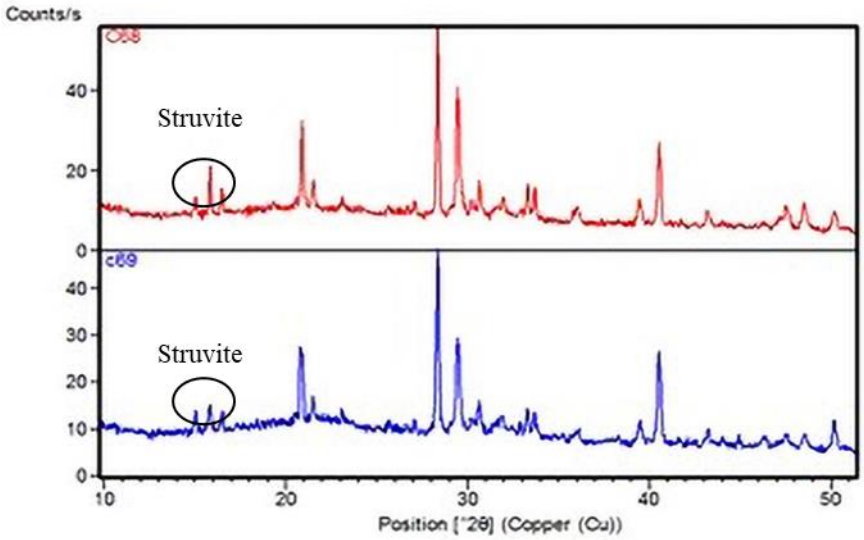

632

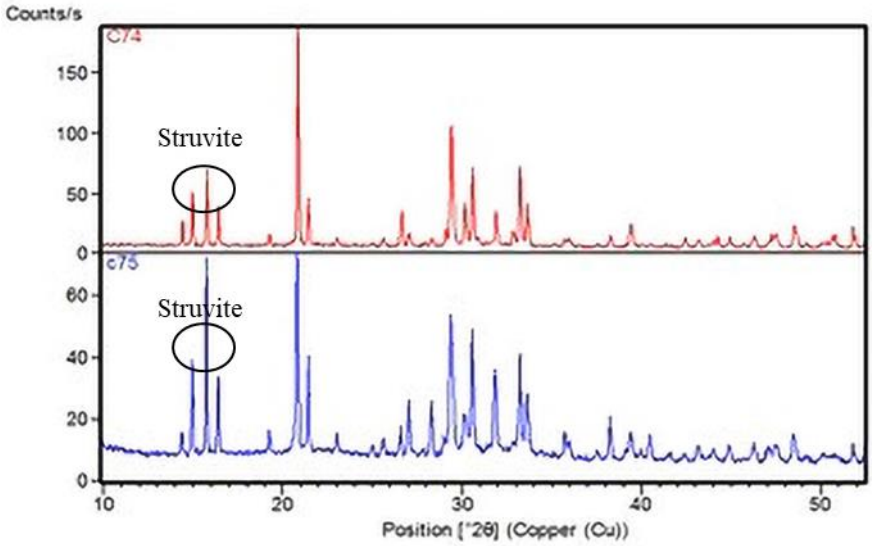

633

634 Figure 3 - Two XRD of the recovered products of Test 2 (up) and Test 4 (bottom)

635

636

637

638

639

640

641

642 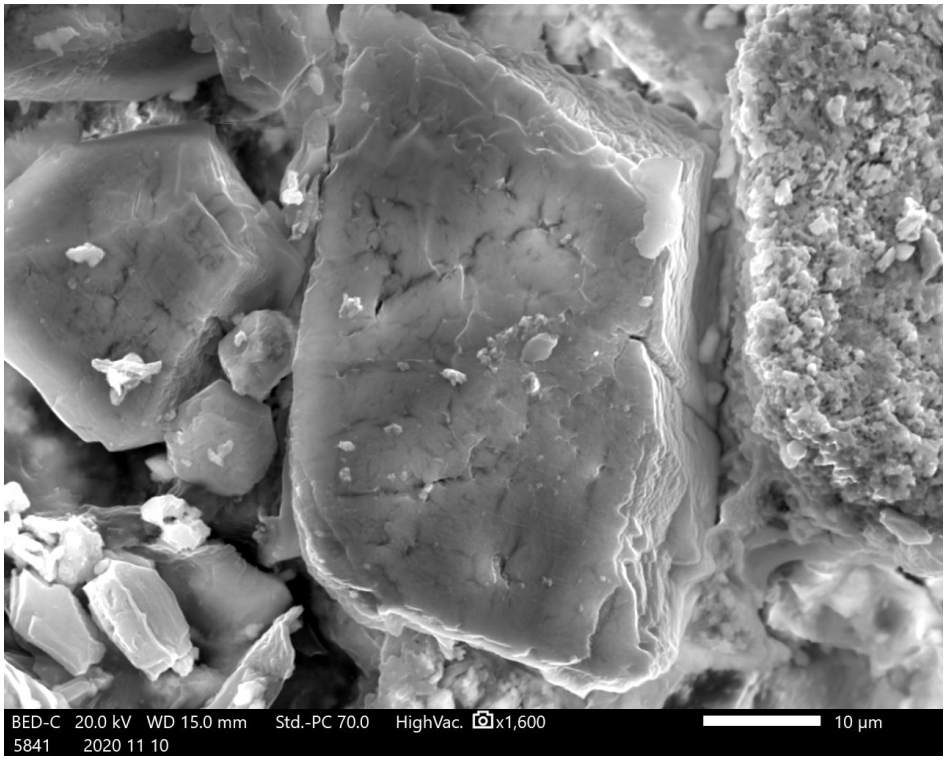

643 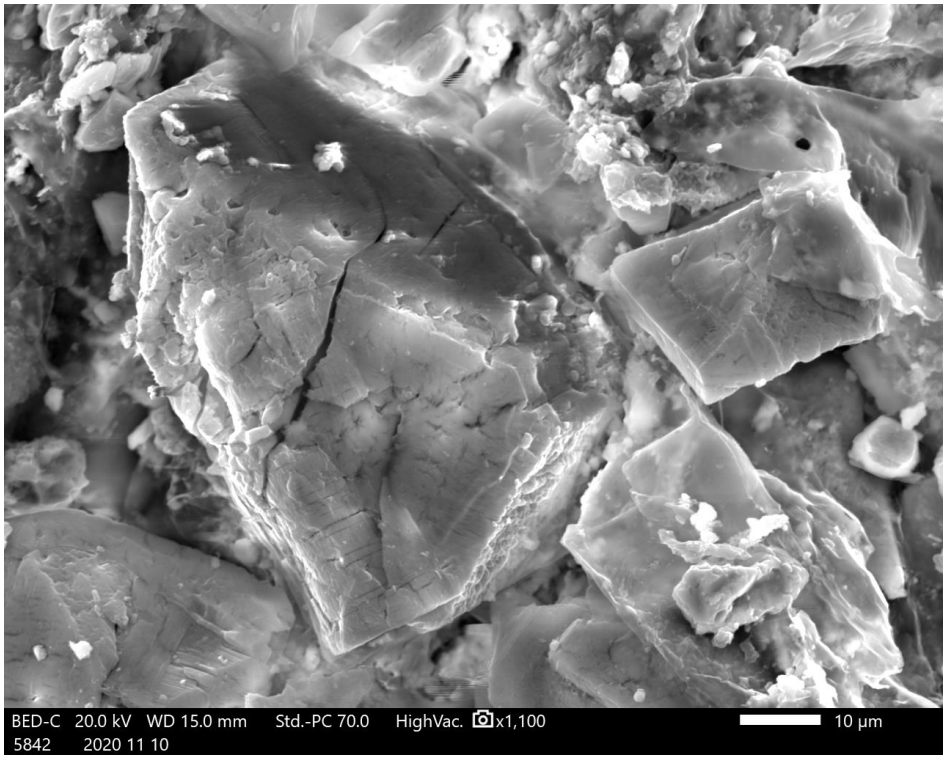

644 Figure 4 - SEM backscattered images of well-formed struvite crystals in Test 4 recovered
645 products.

646

647

648